Electronic Supporting Information for:

Is Electrochemical CO_2 Reduction the Future Technology for Power-to-Chemicals?

Jan Wyndorps, [a] Hesam Ostovari [a] and Niklas von der Assen*[a]

[a] *Institute of Technical Thermodynamics, RWTH Aachen University, 52062 Aachen, Germany*

Phone: +49 241 80 95987
Email: niklas.vonderassen@ltt.rwth-aachen.de

Content

1. Background Processes

Table 1: Summary of background processes and their global warming potentials.

process	reference unit	database process / ecoinvent 3.7 cut-off[1]	global warming potential / kg CO_2-eq.
wind power[1]	kWh	electricity, high voltage//[DE] electricity production, wind, 1-3MW turbine, onshore	0.017
photovoltaic[1]	kWh	electricity, low voltage//[DE] electricity production, photovoltaic, 570kWp open ground installation, multi-Si	0.095
current German grid mix[1]	kWh	electricity, high voltage//[DE] market for electricity, high voltage	0.580
dionized water[1]	kg	water, deionised//[RoW] market for water, deionised	0.000
methanol fossil state-of-the-art[1]	kg	methanol//[GLO] market for methanol	0.625
ethylene fossil state-of-the-art[1]	kg	ethylene, average//[RER] market for ethylene, average	1.396
methanol end-of-life	kg	own calcuation	1.375
ethylene end-of-life	kg	own calcuation	3.143

Table 2: Summary of background processes and their levelized costs.

process	reference unit	database	levelized costs / USD
wind power	kWh	IEA Levelized Costs of Electricity[2]	0.04
photovoltaic	kWh	IEA Levelized Costs of Electricity[2]	0.08
methanol fossil state-of-the-art	kg	Thomson Reuters, Global Data Petrochemical[3]	0.350
ethylene fossil state-of-the-art	kg	Thomson Reuters, Global Data Petrochemical[3]	0.800

2. Correlation CO_2 conversion and Current Density

Figure 1 shows the current status of eCO_2R development. The laboratory experiments are sorted by the current density on the horizontal axis and the single-pass CO_2 conversion on the vertical axis. Increasing current density correlates with increasing single-pass CO_2 conversion. Thus, with further development toward economically feasible current density[4] of ≥ 300 mA/cm^2, we expect the CO_2 conversion to increase.

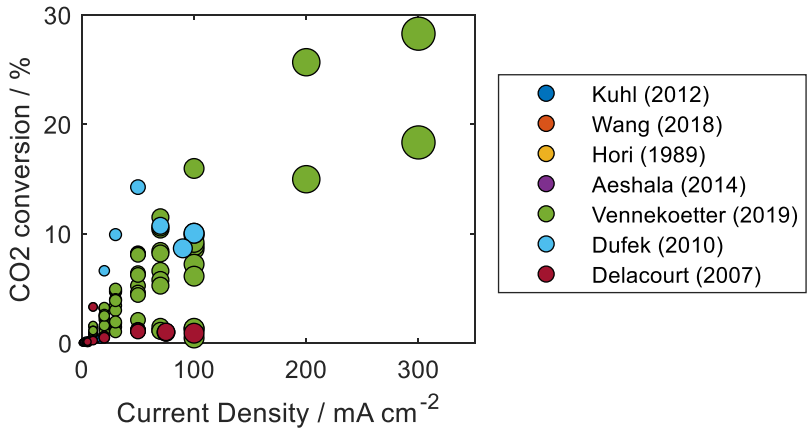

Figure 1: Correlation of single-pass CO_2 conversion and current density in experimental studies.[5–11] The marker size represents the current density.

3. ECO_2R Model

The mass-specific electricity demand of the eCO_2R system is the sum of the energy demand from the electrochemical cell w_{cell} and the separation duty w_{SU} (cf. Eq. 1). The electricity demand of the cell depends on the cell voltage U_{cell} and the faradaic efficiency η_{FE} (cf. Eq. 2) since the electric current I_{cell} can be expressed as a function of the faradaic efficiency (cf. Eq. 3). The Faradaic constant F expresses the electric charge per mole of electrons. The product molecular weight M_p and the required number of electrons z_p are product-specific constants.

$$w_{el} = w_{cell} + w_{SU} \quad \text{(Eq. 1)}$$

$$w_{cell} = \frac{P_{chem}}{\dot{m}_p} = \frac{U_{cell} \cdot I_{cell}}{\frac{\eta_{FE} \cdot I}{z_p \cdot F} \cdot M_p} = \frac{U_{cell} \cdot z_p \cdot F}{\eta_{FE} \cdot M_p} \quad \text{(Eq. 2)}$$

$$I_{cell} = \frac{z_p \cdot F \cdot \dot{m}_p}{\eta_{FE} \cdot M_p} \quad \text{(Eq. 3)}$$

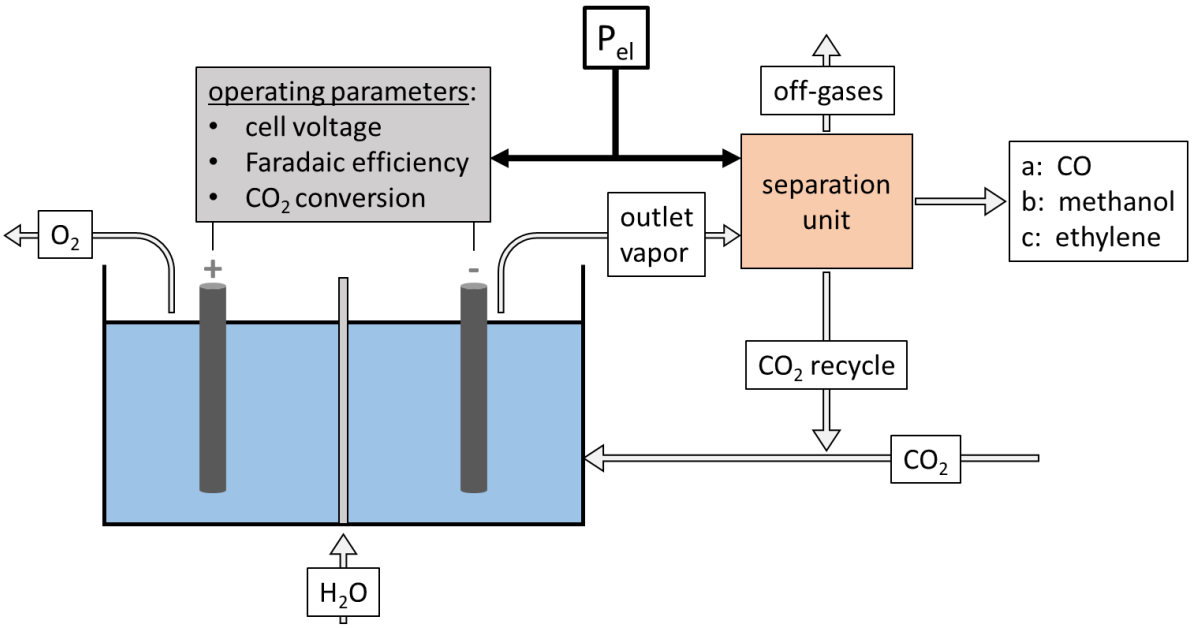

Figure 2: Schematic Illustration of the eCO_2R model that allows calculating the electricity demand P_{el}, the required CO_2, and the required water per kg product (i.e., carbon monoxide (CO), methanol, or ethylene) depending on the variable parameters cell voltage, faradaic efficiency, and single-pass CO2 conversion.

We assume all eCO_2R products to be gaseous under industrial operation temperature of 70-80 °C. Possible electrolyte and liquid product fractions are assumed to be recycled without further treatment or separation. This assumption defines a best-case since enrichment of liquid by-product fractions and pH drift can interfere with the eCO_2R process in alkaline electrolyzers.

The mass-specific separation duty w_{SU} is estimated using the minimal thermodynamic demand based on mixing entropy and ideal gas law. The entropy of the mixed vapor outlet $\dot{S}_{vap}$ is higher than the entropy $\dot{S}_{sep}$ of the three separated streams: product stream (carbon monoxide, methanol, or ethylene), CO_2-recycle, and off-gases. Equation 4 determines the minimal amount of exergy required to overcome the second law of thermodynamics. R defines the universal gas constant. T refers to the ambient temperature of 25 °C.

$$w_{SU} = \frac{P_{SU}}{\dot{m}_p} = \frac{1}{\dot{m}_p} \cdot T \left(\dot{S}_{vap} - \dot{S}_{sep}\right)$$

$$w_{SU} = \frac{1}{\dot{m}_p} \cdot RT \cdot \left[-\sum_c \dot{n}_c^{vap} \ln\left(x_c^{vap}\right) + \sum_c \dot{n}_c^{sep} \ln\left(x_c^{sep}\right)\right] \quad \text{(Eq. 4)}$$

The vapor outlet flows $\dot{n}_c^{vap}$ and its composition x_c^{vap} are a function of faradaic efficiency, CO_2 conversion, electric current, and the by-product distribution factor d_{by}. We do not consider gaseous water or electrolyte fractions in the outlet vapor. The product flow $\dot{n}_p^{vap}$ is determined by the faradaic efficiency and the electric current (cf. Eq. 5). The remaining electric current evolves in by-product formation $\dot{n}_{by}^{vap}$ that is modeled by the distribution factor d_{by} (cf. Eq. 6). We assume a commonly reported by-product distribution with 40 % of the remaining electric current contributing to H_2, 30 % to CO, 10 % to formate, 10 % to methane, and 10 % to ethylene.[12] If the main product is part of the by-product distribution, the by-product distribution is rescaled such that the by-products do not contain the main product. All by-products are regarded as waste and are released into the environment at fully oxidized state (off-gases). We do not consider heat integration from the oxidation of by-products. The

amount of unreacted CO_2 in the vapor outlet $\dot{n}_{CO_2}^{vap}$ can be calculated based on the required CO_2 flow $\dot{n}_{CO_2}^{required}$ and the CO_2 conversion C_{conv} (cf. Eq. 7 & 8).

$$\dot{n}_{p}^{vap} = \frac{\eta_{FE_P} \cdot I}{z_p \cdot F} \quad \text{(Eq. 5)}$$

$$\dot{n}_{by}^{vap} = \frac{d_{by} \cdot (1 - \eta_{FE_P}) \cdot I}{z_{by} \cdot F} \quad \text{(Eq. 6)}$$

$$\dot{n}_{CO_2}^{inlet} = \dot{n}_{CO_2}^{required} + \dot{n}_{CO_2}^{recycle} = \dot{n}_{CO_2}^{required} + \dot{n}_{CO_2}^{vap} \quad \text{(Eq. 7)}$$

$$\dot{n}_{CO_2}^{vap} = \dot{n}_{CO_2}^{inlet}(1 - C_{conv}) = \dot{n}_{CO_2}^{required} \frac{(1 - C_{conv})}{C_{conv}} \quad \text{(Eq. 8)}$$

The required input flows carbon dioxide $\dot{n}_{CO_2}^{required}$ and water $\dot{n}_{H_2O}^{required}$ are calculated based on stoichiometry (cf. Eq. 9 & 10).

$$\dot{n}_{CO_2}^{required} = \sum_{c} \frac{\upsilon_{CO_2}}{\upsilon_c} \dot{n}_c \quad \text{(Eq. 9)}$$

$$\dot{n}_{H_2O}^{required} = \sum_{c} \frac{\upsilon_{H_2O}}{\upsilon_c} \dot{n}_c \quad \text{(Eq. 10)}$$

The equation system is illustrated in Figure 3. The key operating parameters are colored in green, while the orange-colored parameters refer to the eCO2R exchange flows with the chemical background system.

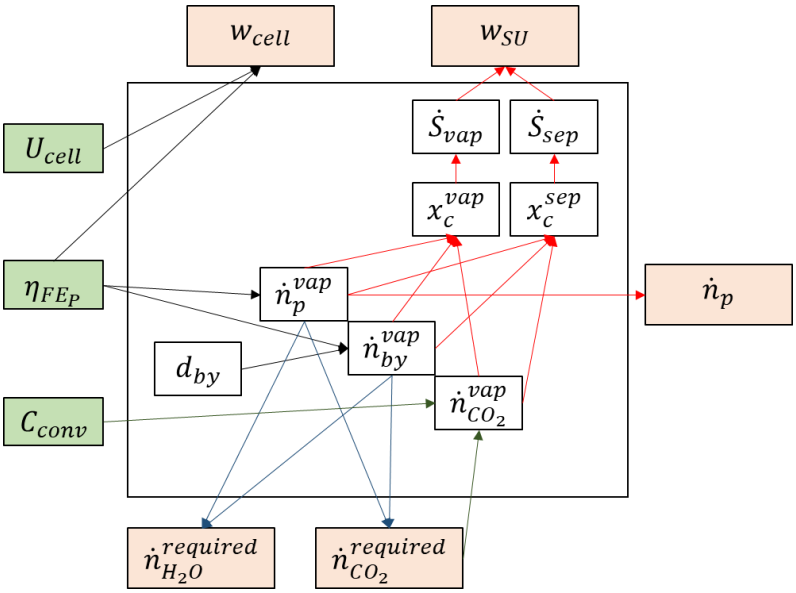

Figure 3: Schematic illustration of the equation system of the eCO₂R model (U_{cell}: cell voltage, η_{FE_P}: faradaic efficiency toward the main product, C_{conv}: CO₂ single-pass conversion, w_{cell}: product-specific electricity demand of the electrochemical cell, w_{SU}: product-specific electricity demand of separation unit, $\dot{n}_{CO_2}^{required}$: required carbon dioxide input flow, $\dot{n}_{H_2O}^{required}$: required water input flow, d_{by}: distribution factor of by-products, $\dot{n}_p^{vap}$: molar product flow in the vapor outlet, $\dot{n}_{by}^{vap}$: molar by-product flows in the vapor outlet, $\dot{n}_{CO_2}^{vap}$: molar flow of unreacted carbon dioxide in the vapor outlet, x_c^{vap}: molar composition of the vapor outlet, x_c^{sep}: molar composition of the separated flows, $\dot{S}_{vap}$: entropy of the vapor outlet, $\dot{S}_{sep}$: entropy of the separated flows).

4. Development requirements for non-ideal separation

Figure 4 shows the effect of non-ideal separation on the development requirements. Figure 4A represents the minimum development requirements when using an ideal separation unit. Figure 4B illustrates the development requirements for a separation unit that requires 10 times the energy of an ideal separation unit. The development requirements are 6 % more ambitious for the faradaic efficiency (from 57.9 % to 61.3 %) and 2 % more ambitious for the cell voltage (from 2.53 V to 2.49 V). Figure 4C shows the development requirements if the separation unit requires 100 times the ideal energy for separation. This results in 44 % more ambitious development requirements for the faradaic efficiency (from 57.9 % to 83.4 %) and 16 % for the cell voltage (from 2.53 V to 2.12 V). The sensitivity analysis shows that inefficient separation processes increase the development requirements for eCO_2R toward low cell voltages and high faradaic efficiencies. Since a study on CO_2 sources[13] reports that the separation units require between 1.5 and 9 times the ideal separation duty, Figure 4B shows reasonable development requirements for eCO_2R to ethylene.

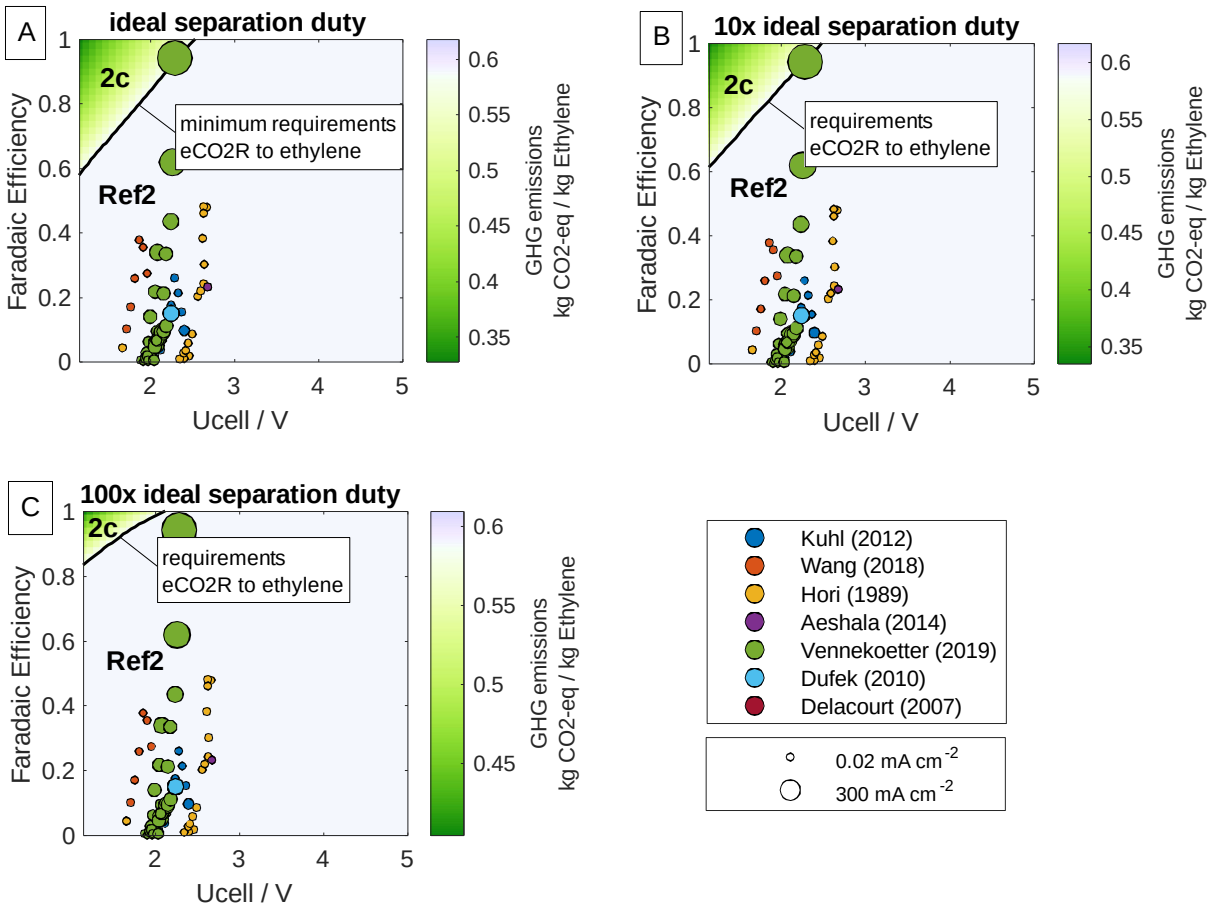

Figure 4: Sensitivity analysis on the effect of non-ideal separation on the development requirement of eCO_2R. (A) shows the minimum development requirement when using an ideal separation unit, (B) represents the development requirements when using 10 times the ideal separation unit, and (C) shows the development requirements when requiring 100 times the ideal separation duty.

5. Economic Feasibility

Next to climate benefits, the eCO_2R pathways could yield economic gains over the H_2-based pathways. The one-step conversion of the direct eCO_2R to MeOH pathway and the direct eCO_2R to ethylene pathway offer reduced plant complexity and geographical independence from chemical production sites for pre- and post-processing. Furthermore, the omission of PEM electrolysis provides potential capital investment savings by using less expensive catalysts for eCO_2R than the noble metals for PEM electrolysis.[14] However, given the different catalysts used for eCO_2R[15] and divers cell construction types[9], a detailed techno-economic assessment remains uncertain and is out of the scope of this study.

In our study, we calculate operating expenditures (OPEX) to illustrate a preliminary techno-economic assessment. Table 3 shows the OPEX per kilogram chemical using wind power with 0.04 USD/kWh.[2] Both the H_2-based pathways and the eCO_2R pathways refer to similar costs and depend highly on electricity costs. The comparison to the fossil-based state-of-the-art technologies shows that power-to-chemicals are almost always more expensive. Currently available H_2-based pathways increase the OPEX by 60-73 %, while best-case H_2-based pathways, operating at equilibrium voltage and 100 % faradaic efficiency, increase the OPEX by only 13-23 %. The best-case eCO_2R pathways range from a -4 % cost reduction to a 54 % cost increase. A detailed techno-economic assessment will further clarify the prospect of eCO_2R and can be the object of future work when higher technology readiness levels are achieved. A detailed assessment should also consider environmental policies, e.g., CO_2 taxes or emission trading schemes, which can render power-to-chemical pathways more competitive over the CO_2-intensive fossil routes.

Table 3: Comparison of OPEX per kilogram chemical of the fossil-based state-of-the-art technologies, the H_2-based pathways, and the eCO_2R pathways (in US Dollar/ton). Best-case implicates operation at equilibrium potential and 100 % faradaic efficiency. The relative reduction potentials refer to the fossil-based state-of-the-art.

OPEX	**Fossil state of the art**[3]	**Wind-powered power-to-chemicals**				
		H_2-based (Ref)	**H_2-based (best-case)**	**best-case eCO_2R to CO (a)**	**best-case eCO_2R to methanol (b)**	**best-case eCO_2R to ethylene (c)**
methanol (1)	350 USD/t	560 USD/t (+60 %)	395 USD/t (+13 %)	494 USD/t (+41 %)	346 USD/t (-1 %)	
ethylene (2)	800 USD/t	1,386 USD/t (+73 %)	986 USD/t (+23 %)	1,228 USD/t (+54 %)	863 USD/t (+7 %)	772 USD/t (-4 %)

References

1 Gregor Wernet, Christian Bauer, Bernhard Steubing, Jürgen Reinhard, Emilia Moreno-Ruiz and Bo Weidema, The ecoinvent database version 3 (part I): overview and methodology, *Int J Life Cycle Assess*, 2016, **21**, 1218–1230.

2 IEA, Levelised Cost of Electricity Calculator, https://www.iea.org/articles/levelised-cost-of-electricity-calculator, (accessed 6 September 2021).

3 Thomson Reuters, Global Data Petrochemical, https://emea1.apps.cp.thomsonreuters.com/web/cms/?navid=20365, (accessed 5 January 2021).

4 Colin Oloman and Hui Li, Electrochemical Processing of Carbon Dioxide, *ChemSusChem*, 2008, **1**, 385–391.

5 Kendra P. Kuhl, Etosha R. Cave, David N. Abram and Thomas F. Jaramillo, New insights into the electrochemical reduction of carbon dioxide on metallic copper surfaces, *Energy & Environmental Science*, 2012, **5**, 7050–7059.

6 L. Wang, S. A. Nitopi, E. Bertheussen, M. Orazov, C. G. Morales-Guio, X. Liu, D. C. Higgins, K. Chan, J. K. Nørskov, C. Hahn and T. F. Jaramillo, Electrochemical Carbon Monoxide Reduction on Polycrystalline Copper: Effects of Potential, Pressure, and pH on Selectivity toward Multicarbon and Oxygenated Products, *ACS Catal.*, 2018, **8**, 7445–7454.

7 Y. Hori, A. Murata and R. Takahashi, Formation of hydrocarbons in the electrochemical reduction of carbon dioxide at a copper electrode in aqueous solution, *J. Chem. Soc., Faraday Trans. 1*, 1989, **85**, 2309.

8 L. M. Aeshala, R. Uppaluri and A. Verma, Electrochemical conversion of CO_2 to fuels: tuning of the reaction zone using suitable functional groups in a solid polymer electrolyte, *Physical chemistry chemical physics : PCCP*, 2014, **16**, 17588–17594.

9 J.-B. Vennekoetter, R. Sengpiel and M. Wessling, Beyond the catalyst: How electrode and reactor design determine the product spectrum during electrochemical CO2 reduction, *Chemical Engineering Journal*, 2019, **364**, 89–101.

10 Eric J. Dufek, Tedd E. Lister and Michael E. McIlwain, Bench-scale electrochemical system for generation of CO and syn-gas, *J Appl Electrochem*, 2011, **41**, 623–631.

11 Charles Delacourt, Paul L. Ridgway, John B. Kerr and John Newman, Design of an Electrochemical Cell Making Syngas (CO + H2) from CO2 and H2O Reduction at Room Temperature, *J. Electrochem. Soc.*, 2007, **155**, B42.

12 S. Nitopi, E. Bertheussen, S. B. Scott, X. Liu, A. K. Engstfeld, S. Horch, B. Seger, I. E. L. Stephens, K. Chan, C. Hahn, J. K. Nørskov, T. F. Jaramillo and I. Chorkendorff, Progress and Perspectives of Electrochemical CO2 Reduction on Copper in Aqueous Electrolyte, *Chemical Reviews*, 2019, **119**, 7610–7672.

13 N. von der Assen, L. J. Müller, A. Steingrube, P. Voll and A. Bardow, Selecting CO2 Sources for CO2 Utilization by Environmental-Merit-Order Curves, *Environmental science & technology*, 2016, **50**, 1093–1101.

14 K. Bareiß, C. de La Rua, M. Möckl and T. Hamacher, Life cycle assessment of hydrogen from proton exchange membrane water electrolysis in future energy systems, *Applied Energy*, 2019, **237**, 862–872.

15 G. O. Larrazábal, A. J. Martín and J. Pérez-Ramírez, Building Blocks for High Performance in Electrocatalytic CO2 Reduction: Materials, Optimization Strategies, and Device Engineering, *The journal of physical chemistry letters*, 2017, **8**, 3933–3944.